Algebraic instability in shallow water flows with horizontally nonuniform density

V. P. Goncharov[1] and V. I. Pavlov[2]

[1]*A. M. Obukhov Institute of Atmospheric Physics RAS, 109017 Moscow, Russia*

[2]*UFR des Mathématiques Pures et Appliquées - LML CNRS UMR 8107, Université de Lille 1, 59655 Villeneuve d'Ascq, France*

(Received 25 November 2014; published 6 April 2015)

The regimes and mechanisms of the Rayleigh-Taylor instability have been studied in the scope of the nonhydrostatic shallow water model with horizontally nonuniform density. As analysis shows, the nonhydrostaticity has a crucial influence on the instability. It is for this reason that at the final stage a collapse tendency predicted on the base of the hydrostatic scenario slows down and turns into the regime of algebraic instability. The numerical testing has shown that in spite of its simplicity, the model is quite able to describe realistically a number of effects. For example, the model captures the shallowing effect, which manifests itself as profile concavities on either side of the jet coming out of the boundary layer.

DOI: 10.1103/PhysRevE.91.043004 PACS number(s): 47.20.Cq, 47.10.Df, 47.20.Ma

I. INTRODUCTION

The main aim of this work is to discard the hydrostatic approximation in the shallow water (SW) model with horizontally nonuniform density and to revise scenarios describing the final stage of the Rayleigh-Taylor instability in this model.

The classic Rayleigh-Taylor instability occurs when a fluid with lower density accelerates a fluid of higher density, or when a higher density fluid is positioned above a fluid with lower density in a gravitational field or in an accelerating frame of reference. It is a dynamic process where the two fluids seek to reduce their combined potential energy. An initial perturbation (of small magnitude) of the interface between fluids starts in the exponential regime (described by linear differential equations for interface deformation), proceeds to the nonlinear regime, and finally enters a turbulent regime where multiple space scales emerge. Understanding of the dynamics of this process is crucial to the understanding of many phenomena of combustion processes in astrophysical and geophysical environments, the inertial (laser) fusion, accelerating medium of variable density, two-phase flows, and many other phenomena.

Extensive literature on the Rayleigh-Taylor instability exists (see for example Refs. [1–7] and references therein). In the main, it consists of numerous numerical investigations. In this context, the important question appears about a classification of parameters for possible regimes of evolution, which is not taken into consideration in some works.

One should distinguish between two limit cases based on the ratio of thickness h of the active fluid layer (significantly smaller than vertical size of the container) and the characteristic space scale of initial horizontal deformation of the interface k^{-1} (of order the horizontal size of the container): deep $kh \gg 1$ and shallow $kh \ll 1$ fluids.

In the case of $kh \gg 1$, a small initial single-mode (sinusoidal) deformation of deep fluid interface $\delta h(x,0) \sim \sin kx$ with $kh(x,0) \ll 1$ initially grows as $\delta h(x,t) \simeq \delta h(x,0) \exp \Gamma t$ with the growth rate (for a single-mode k) $\Gamma = \sqrt{Agk}$ (when one neglects surface tension). Here, g is the gravity or inertial acceleration directed from the h fluid to l fluid, dimensionless parameter $A = (\rho_h - \rho_l)/(\rho_h + \rho_l) > 0$ is the Atwood number, ρ_h and ρ_l are densities of heavier and lighter fluids, respectively, and $\delta h(x,0)$ is the initial magnitude of single-mode perturbation. When the initial deformation of the interface is not single mode, in the regime with exponential growth each perturbation mode develops independently and is described by linear instability theory [8]. As the deformation of the interface becomes large, $k\delta h(x,t) \simeq 1$, the fluid interface is transformed prior to transitioning to the turbulent regime of the interface motion into spikes (where the heavier fluid penetrates the lighter fluid) and bubbles (where the lighter fluid rises into the heavier fluid).

In this work we focus attention on the other limit case, the so-called shallow-water-like approximation (SWL) with $kh \ll 1$. The SWL approximation arises in many physical situations when the characteristic horizontal scale perpendicular to the imposed external (for example, gravity) acceleration $\mathbf{g}$ is much larger than the vertical dimension of the flow, or when the collinear to $\mathbf{g}$ component of fluid velocity is strongly suppressed for some reason. In this case, the fluid dynamic description can be drastically simplified, permitting the use of simplified models.

In theoretical investigations, the simplest, so-called hydrostatic, approximation is frequently used when the vertical component of velocity in active layer is suppressed or is neglected, $w = 0$, and the horizontal one is independent on vertical coordinate z.

According to recent studies [9–11], the Rayleigh-Taylor instability in the hydrostatic approximation has a blow-up behavior, which leads to the formation of singularities during a finite time, or, in other words, to the collapse. The situation becomes more complicated when the hydrostatic balance is violated to the point that proper corrections must be made to take into account nonlinear dispersion whose mechanism begins to come into play.

In SW models with free boundaries, this problem is solved by using the so-called Green-Naghdi correction [12–16]. In the case of potential flows, the same task can be solved in the framework of the Hamiltonian approach, for which the nonlinear dispersion, following from the effect of nonhydrostaticity, can be obtained in any order of perturbation theory [17–22].

As far as we know, for the SW models with large-scale horizontally nonuniform density, similar studies have not been conducted. Although quite apparently the flow behavior in final stages of the instability is a highly topical problem. Its

study provides a way for an understanding of the different important processes, for example, the vertical mixing in many physical applications, including nuclear physics, astrophysics, atmospheric and ocean sciences.

To understand some features of the Rayleigh-Taylor instability, we consider the simplest statement—unbounded incompressible fluid with a density jump, characterized by the Atwood's number A. Suppose that the main dimensional parameters of the problem are: gravity acceleration g; the magnitude (peak) of interface deformation h; its initial value h_0; the current time t; and the characteristic interval of possible singularity formation t_0 (see below, in the main text). Thus, $h = h(t,g,t_0,h_0,A)$.

On the dimensional analysis grounds, only the three-argument functional dependence $h = h_0 F(gt^2/h_0, t_0/t, A)$ is admitted. At large time $t \gg t_0$, the second argument tends to zero. In this case, the system must forget its initial state and dependence on h_0 must disappear. This is possible only if the function F is linear in the first argument. Thus, these qualitative arguments lead us to the relation $h \sim gt^2 f(A)$. Such instability in physics is called algebraic [23] unlike collapse, which develops within a finite time t_0 according to the law $h \sim (t_0 - t)^\alpha$, $\alpha < 0$.

However, the scale invariance does not explain everything. For example, from this point of view one cannot account for why bubbles forming between jets move with constant velocity. The number of open questions becomes considerably larger if we consider more general models [24], which use other boundary and initial conditions and take into account effects of viscosity, diffusion, thermal and electric conduction. All these reasons lead to the violation of the scale invariance $L \sim gT^2$ for typical scales of length L and time T and hence to the occurrence of new typical scales of motion.

The existence of unstable regimes and lack of their preliminary classification in the parameter space frequently leads to situations when the numerical simulation for such models is faced with large difficulties. Considerable efforts and time are required to distinguish effects of real (physical) instability from numerical ones and to separate them. In this respect, analytical methods have substantial advantages.

The study of blow-up instability (collapse) [25] shows that even in the absence of exact solutions, using only the integral criteria, analytical methods are able to provide a deep qualitative understanding of behavior of unstable nonlinear systems. It is evident, however, that these goals cannot be attained without the development of adequate models.

In this paper, we by no means intend to develop one more large-scale version of the model. Our aim is to find a parametrization that works effectively at large and small scales in the context of the Rayleigh-Taylor instability. The importance of the issue becomes clear in the following historical episode.

The well-known Manhattan Project required implementation of a simultaneous and uniform explosive compression of a spherical target of density ρ_h by a spherical layer of less dense ρ_l for which the Atwood number was small, notably $A \leqslant 0.01$. This is how the implosion was created.

Physically, the behavior of the matter near the ρ_h/ρ_l interface, which during compression moves locally with acceleration, is equivalent to the behavior of a fluid (subject to the homogeneous gravity of Earth) in a drinking glass quickly turned upside down. In such a situation, the initial interface is obviously unstable with respect to spontaneous small perturbation of the jump density interface (Rayleigh-Taylor instability) and quickly deforms producing spikes and fingers (mutual interpenetration of the heavy/light fluid into the light/heavy fluid).

Such a problem is ill posed in the sense of rigorous mathematics working usually with stable solutions. However, for the success of the entire Project it was critically important to determine the conditions under which these fingers and spikes develop slower than the rapidity of the implosion. Otherwise, instead of a powerful explosion one would get a trivial whiff.

Fermi and von Neumann were instrumental in analyzing this problem. Their goal was attained by using a beautifully simple and elegant model based on the Lagrangian approach. In particular, as one of the most important results for the Project realization, they found the growth rate for the magnitude of the surface deformation in the nonlinear regime of evolution. It turned out that the time dependence of the instability evolution growth is proportional to the square of time (not exponential or blow-up). In the end, as we all know, this result was successfully implemented in the Project [26,27].

The field theory abounds with examples when motion equations are unsolvable or even absent. In this case, the key role belongs to symmetry principles. Therefore, one of the important problems is to reveal these symmetries. But the inverse problem of constructing models with given symmetries is not less important. In this case, the symmetry principles act as selection rules, which extract from a set of admissible models only those that possess the required properties.

If there are physical reasons to assume that only some symmetries and corresponding constraints are the most important and it is they that are responsible for the key features of the behavior of the system, then there is a ready-made recipe for the construction of a minimal (simplified) model. In practice, this is being reached by means of the Hamiltonian or Lagrangian approach [28] and due to symmetry reduction, as a rule, leads to simpler equations. The works of Fermi-Neumann [26,27] are an impressive example in this regard.

As a constraint, just like these authors, we use the incompressibility condition. The main difference is that for eliminating this constraint we employ the parametrization of the velocity field while Fermi and von Neumann use for this the parametrization of the interface. Another distinction is purely technical and consists in that in order to derive the equations of motion, we apply the Hamiltonian approach based on hydrodynamic Poisson brackets. This tool was not yet known in Fermi-Neumann's times.

Minimal models are a formalization of the Occam's razor principle, which says that "entities are not to be multiplied beyond necessity" [29]. Scale invariance for minimal models is a rather typical property that implies the existence of self-similar solutions. Being intermediate asymptotics of nondegenerate problems [30], these solutions are very useful in studying the final stages of strongly nonlinear processes, when the system forgets about details related to the initial data and its behavior fully depends on the motion integrals. For unstable strongly nonlinear systems, the existence of self-similar solutions is also the important fact since they play a role of structural

elements of which the asymptotics of the Cauchy problem at $t \to \infty$ can be made. It is worth noting that such solutions are in some sense like solitons.

Usually, the minimal models are arranged so that they could describe the large-scale processes at a good level. So if in an initial state along with large scales there also exist small ones, the small-scale turbulence will develop increasingly with the lapse of time, masking the large-scale structures. This means, to ensure the efficiency of these models for unstable regimes, their initial states should not be excessively detailed.

Besides studying of blow-up instability [25], self-similar solutions are also useful for researching of a strong large-scale turbulence, sometimes called structural. In particular, the self-similar solutions found for the model in the hydrostatic approximation were used for explaining a scaling in turbulent spectra of Sun's supergranulation [31].

This paper is organized as follows. In Sec. II we discuss the model setup and formulate the governing equations in nonhydrostatic SW approximation with horizontal density gradients. In Sec. III we analyze self-similar solutions and consider possible scenarios of their behavior. Sec. IV is devoted to the paradox of superacceleration. This paradox owes its origin to Fermi, in whose opinion the spikes (penetration of the heavy fluid into the light fluid) cannot be moving with acceleration greater than the Archimedes acceleration. Numerical testing of the model is performed in Sec. V. One of our aims in this section is to demonstrate the shallowing effect in the course of the development of the Rayleigh-Taylor instability in the planar horizontally nonuniform boundary layer. In Sec. VI we summarize our results. Appendix A gives detailed motivation of the used model and lists additional relevant data that we hope are useful for the most inquisitive readers.

II. FORMULATION OF MODEL

We consider a two-dimensional field model whose evolution is governed by the equations

$$\partial_t \mathbf{u} + (\mathbf{u}\cdot\nabla)\,\mathbf{u} = -\frac{1}{2h}\nabla(h^2\tau) - \frac{1}{3h}\nabla\left(h^2\frac{d^2h}{dt^2}\right), \qquad (1)$$

$$\partial_t h + \nabla\cdot(h\mathbf{u}) = 0, \quad \partial_t \tau + \mathbf{u}\cdot\nabla\tau = 0. \qquad (2)$$

These equations describe the depth-averaged flow in the active (lower) layer in nonhydrostatic SW approximation and can be formulated within the framework of the two-layer model that is shown in Fig. 1. This model (see the Appendix for more details) supposes that two incompressible fluids with densities $\varrho_0 = \text{const}$ and $\varrho_0 + \Delta\varrho(\mathbf{x},t)$ are separated by the interface $z = h(\mathbf{x},t)$ and contained between two rigid parallel planes $z = 0$ and $z = l$ under action of gravity g. The other notations are as follows: $\mathbf{x}$ are the Cartesian horizontal coordinates; ∇ is the horizontal gradient operator; ∂_t and d/dt are the partial and total time derivatives; $\mathbf{u}(\mathbf{x},t)$ is the depth-averaged horizontal velocity in the active layer, $\tau(\mathbf{x},t) = g\Delta\varrho/\varrho_0$ is the relative buoyancy, which, unlike h, may take any sign.

In the simplest case $\tau = g = \text{const}$, Eqs. (1)–(2) are reduced to the well-known Green-Naghdi equations, which describe gravity waves on the surface of shallow water in the nonhydrostaticity approximation [12–16]. If the hydrostatic balance is broken sufficiently weakly, there is every reason

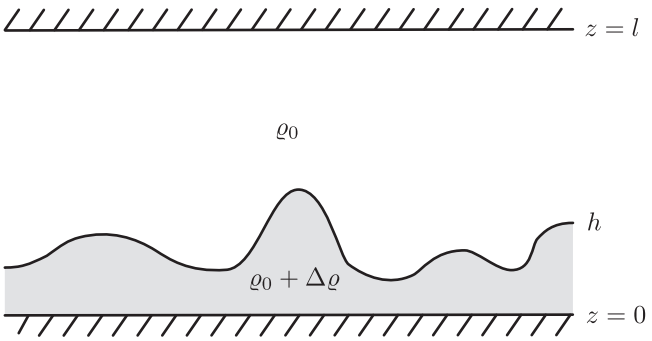

FIG. 1. The model of the active (lower) layer with horizontally nonuniform density.

to ignore the Green-Naghdi correction—the last term in Eq. (1). It is in this approximation that Eqs. (1)–(2) were used to study the development of the Rayleigh-Taylor instability in large-scale flows with horizontally nonuniform density [9–11]. Nevertheless, the model (1)–(2) is not a generalization of Ripa-type models [32] in the strong sense of this word. Rather, it is a parametrization composed of terms, which dominate at the initial and final stage of the Rayleigh-Taylor instability.

Equations (1)–(2) can be derived from first principles and follow from the Hamiltonian formulation [28,33–35] of the two-dimensional motion of a nonbarotropic gas with the Hamiltonian

$$H = \frac{1}{2}\int\left(h\mathbf{u}^2 + \frac{1}{3}h^3(\nabla\cdot\mathbf{u})^2 + h^2\tau\right)d\mathbf{x}. \qquad (3)$$

See the Appendix for more details about their derivation.

Besides the Hamiltonian H, Eqs. (1)–(2) conserve integrals

$$\mathbf{P} = \int h\mathbf{u}d\mathbf{x}, \quad M = \int h\,(\mathbf{x}\times\mathbf{u})\,d\mathbf{x}, \qquad (4)$$

$$C = \int h(F_1(\tau) + q\,F_2(\tau))d\mathbf{x}. \qquad (5)$$

The physical significance of $\mathbf{P}$ and M are respectively the total linear and angular momentum. The last integral C is nothing else than an annihilator (Casimir) for the Poisson brackets [32], F_1 and F_2 are arbitrary functions of the buoyancy τ. The quantity q is the generalized vorticity defined as [36,37]

$$q = \frac{1}{h}\nabla\times\left(\frac{\mathbf{m}}{h}\right) \quad \mathbf{m} = \frac{\delta H}{\delta\mathbf{u}} = h\mathbf{u} - \frac{1}{3}\nabla(h^3\nabla\cdot\mathbf{u}),$$

where $\mathbf{m}$ is the momentum density. Note that q obeys the equation

$$\partial_t q + \mathbf{u}\cdot\nabla q = \frac{1}{2h}\,(\nabla h\times\nabla\tau)\,,$$

and hence is an advected quantity only if $\tau = \text{const}$.

Putting $F_1 = \{1,\tau\}$ and $F_2 = 0$, in what follows, we will use in addition to M two more integrals

$$Q = \int h d\mathbf{x}, \quad N = \int h\tau d\mathbf{x},$$

which have meaning of the total volume and the total buoyancy, respectively.

III. SELF-SIMILAR SOLUTIONS

In the radial symmetric case, Eqs. (1)–(2) look as follows:

$$\partial_t u + u\partial_r u - \frac{1}{r}v^2 = -\frac{1}{h}\partial_r\left(\frac{1}{2}h^2\tau + \frac{\epsilon}{3}h^2\frac{d^2h}{dt^2}\right), \quad (6)$$

$$\partial_t v + u\partial_r v + \frac{1}{r}uv = 0, \quad (7)$$

$$\partial_t h + \frac{1}{r}\partial_r(rhu) = 0, \quad \partial_t\tau + u\partial_r\tau = 0, \quad (8)$$

where u and v are the radial and azimuthal components of velocity, respectively, and $\epsilon = (1,0)$ is the on/off parameter of nonhydrostaticity.

Just like in the hydrostatic model [11], Eqs. (6)–(8) possess exact self-similar solutions

$$h = \frac{h_0}{\beta^2}\left(1 - \frac{r^2}{\beta^2}\right)^{1/2}, \quad \tau = \tau_0\left(1 - \frac{r^2}{\beta^2}\right)^{1/2} \quad (9)$$

$$u = \frac{\alpha}{\beta}r, \quad v = \frac{c}{\beta^2}r. \quad (10)$$

Here $\alpha(t)$, $\beta(t)$ are time-dependent functions which must be found, and constants h_0, τ_0, c are fixed by the integrals of motion

$$h_0 = \frac{3Q}{2\pi}, \quad \tau_0 = \frac{4N}{3Q}, \quad c = \frac{5M}{2Q}.$$

Substituting of (9), (10) into (6)–(8), after nondimensionalization with the characteristic length, L, and time, T, such that

$$L = 2^{-1/6}\left(\frac{3Q}{\pi}\right)^{1/3}, \quad T = \frac{\sqrt{\pi}L^2}{\sqrt{|12N + 25\pi M^2/Q^2|}},$$

we get

$$\frac{d\alpha}{dt} = \frac{3\epsilon\alpha^2 + \frac{\sigma}{4}\beta^4}{\beta(\epsilon + \beta^6)}, \quad \frac{d\beta}{dt} = \alpha. \quad (11)$$

Here σ is the sign function defined as

$$\sigma = \begin{cases} 1 & \text{for } \kappa > 0 \\ 0 & \text{for } \kappa = 0 \\ -1 & \text{for } \kappa < 0 \end{cases}, \quad \kappa = 12N + 25\pi\frac{M^2}{Q^2}.$$

Equations (11) conserve the integral of energy

$$E = \frac{\alpha^2(\epsilon + \beta^6)}{2\beta^6} + \frac{\sigma}{8\beta^2}, \quad (12)$$

and can be rewritten in the form

$$\frac{d\alpha}{dt} = -\frac{\beta^6}{\epsilon + \beta^6}\frac{\partial E}{\partial\beta}, \quad \frac{d\beta}{dt} = \frac{\beta^6}{\epsilon + \beta^6}\frac{\partial E}{\partial\alpha}. \quad (13)$$

Depending on the sign of κ, the system (11) has two dynamic regimes. The instability is possible only if $\kappa \leqslant 0$ and hence $N \leqslant -\frac{25}{12}\pi(M/Q)^2$. Phase trajectories for this case are presented in Fig. 2. The dashed line corresponds to $E = 0$ and separates closed phase trajectories with $E < 0$ from unclosed ones with $E > 0$. Note that, irrespective of the sign of the energy E, all trajectories approach the critical point

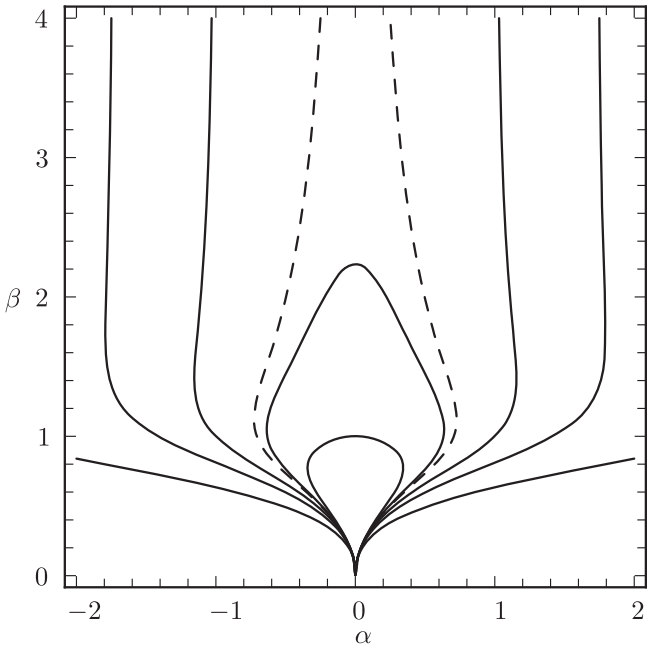

FIG. 2. Phase portrait of the nonhydrostatic model in the regime of instability $\kappa < 0$.

$(\alpha = 0, \beta = 0)$ in the vicinity of which the system behaves unstably.

The hydrostaticity regime is possible in an initial stage of instability as long as the inequality $\beta(0) \geqslant \beta \gg 1$ holds true. In this case, assuming $\epsilon = 0$, from Eqs. (11) one can find the collapsing solution (see Refs. [9,10])

$$\beta = (t_0 - t)^{1/2}, \quad (14)$$

where t_0 is a collapse time.

As shown in Fig. 3, this solution remains valid also for $\epsilon = 1$ until β approaches 1. After the variable β becomes so small that $\beta \ll 1$ there comes the final stage when the instability can be approximated reasonably closely by the equation

$$\frac{d^2\beta}{dt^2} = \frac{3}{\beta}\left(\frac{d\beta}{dt}\right)^2 - \frac{1}{4}\beta^3. \quad (15)$$

This equation has the solution

$$\beta = 2t^{-1}, \quad (16)$$

from which in the special case $M = 0$, returning to dimensional quantities, we obtain

$$h_{\max} = h_0\beta^{-2} \approx \tfrac{3}{4}\tau_0 t^2. \quad (17)$$

Because, in the approximation $\Delta\varrho/\varrho_0 \ll 1$, the Atwood parameter A and the buoyancy τ are linearly locally connected as

$$\tau \approx 2Ag, \quad (18)$$

the relation (17) can be rewritten in the form

$$h_{\max} = h_0\beta^{-2} \approx \tfrac{3}{2}A_0 g t^2, \quad (19)$$

where $A_0 = \tau_0/(2g)$ is the peak value of the Atwood parameter.

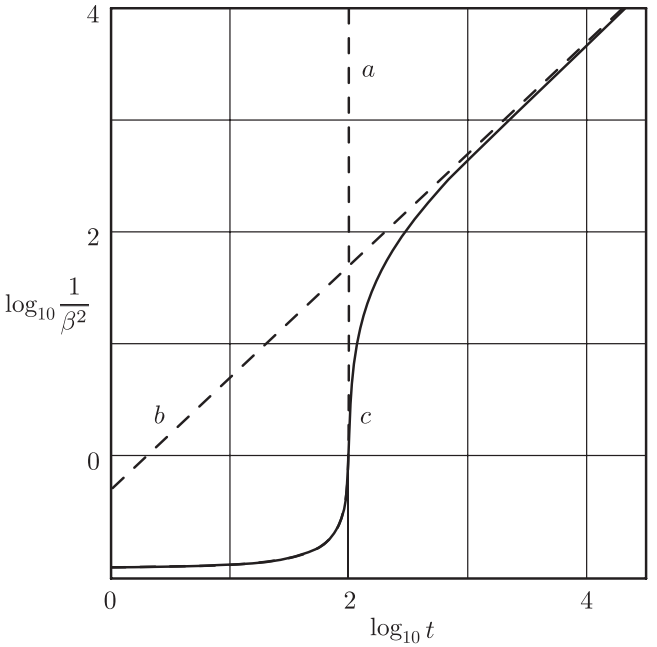

FIG. 3. The solid curve (c) describes the transition from the collapsing regime to the regime of algebraic instability. The initial asymptotics (a) corresponds to the collapsing solution (14) while the solution (16) gives the final asymptotics (b).

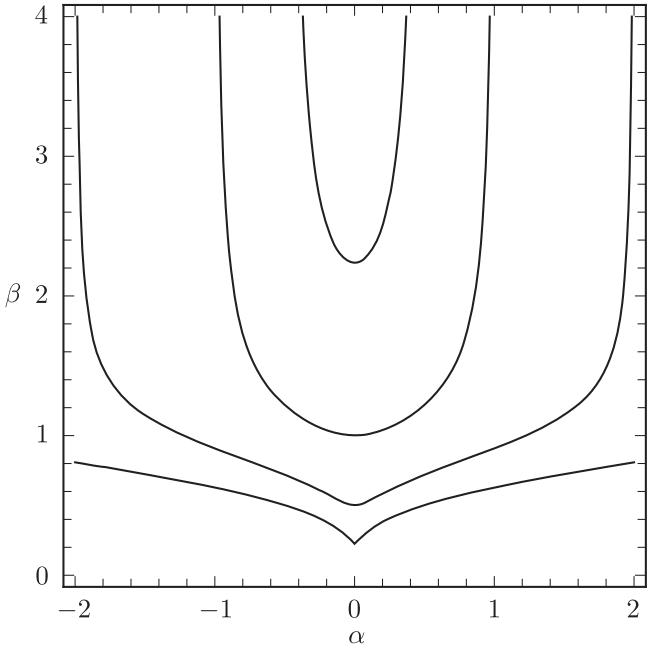

FIG. 4. Phase portrait of the nonhydrostatic model in the regime of stability $\kappa > 0$.

The power-law growth with time says that in the final stage the regime of blow-up instability predicted for hydrostatic models [9–11] slows down and turns into the regime of algebraic instability (secular behavior). In particular Eq. (17) means that the jet formed of a light fluid moves upward with the constant acceleration $3gA_0$. By comparison, Fermi's model [27] gives the similar result but with the coefficient $\frac{16}{7}$ in front of the gravity acceleration g.

Note that if $\kappa < 0$ and $E < 0$ the limiting regime (16) is the only possible for all initial data. But if $E > 0$, one more limiting regime

$$\beta \approx \sqrt{2Et}, \quad \alpha \approx \sqrt{2E}, \tag{20}$$

is also possible as $t \to \infty$. It is not difficult to surmise that if the law (16) is treated as the formation of an infinitely narrow jet, then the law (20) describes an inverse process of how the jet spreads out over a plane boundary.

In the stable regime, when $\kappa > 0$, the motion can occur only if $E > 0$. Moving along open trajectories as shown in Fig. 4, the system (11) has the same trivial asymptotes as (20).

IV. SUPERACCELERATION EFFECT

The superacceleration is understood as an effect when the vertical acceleration of a fluid parcel exceeds the gravitational acceleration. Fermi [26] was the first who paid attention to this phenomenon in the context of the Rayleigh-Taylor instability at the interface. Considering jointly with von Neumann [27] the planar model and schematizing the surface shape as indicated in Fig. 5, they introduced parameters $x(t)$, $y(t)$, $z(t)$ which, due to incompressibility, are related with each other by the relation $y(1 - z) = xz$. The equations of motion were derived with the use of the Lagrangian approach and resulted in the following asymptotic expression

$$x \approx \frac{8}{7}\frac{A}{1+A} g t^2,$$

where $A = (\varrho - \sigma)/(\varrho + \sigma)$ is the Atwood number, ϱ, σ are different constant densities, and $\varrho > \sigma$, so $0 \leqslant A \leqslant 1$. Thus,

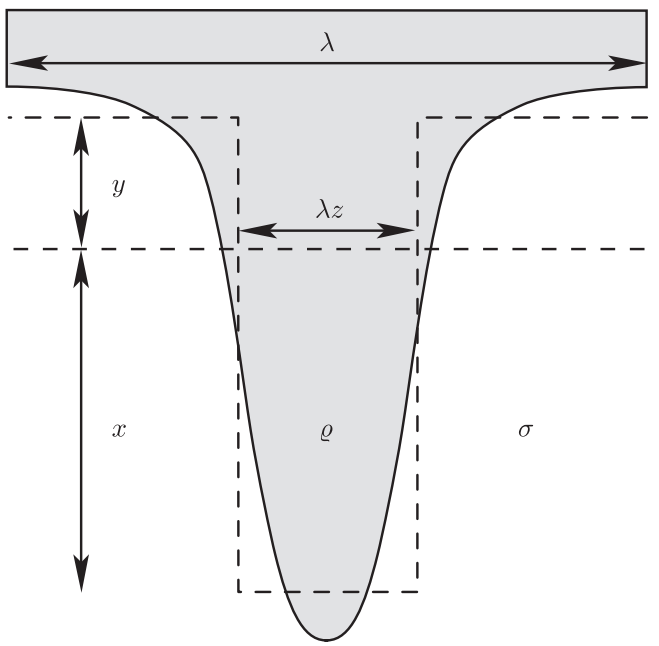

FIG. 5. Profiles of the interface over the period λ in the model [27]. The real profile is shown by solid curve, the polygonal dashed line corresponds to the schematic profile while the central dashed line is the unperturbed interface location.

the tip of the downward jet falls in vacuum ($A = 1$) with acceleration equal to $\frac{8}{7}g$.

Fermi explained the effect of superacceleration ($\frac{8}{7} > 1$) by the crudeness of the model. However, in our opinion this effect is physically quite possible and should not cause a big concern. Indeed, in all points of the flow except the center of masses (or centroid), the pressure gradient along with external forces (in our case it is Archimedes force) give a contribution to the acceleration. The single point, where this contribution vanishes, is the centroid. Therefore, here there can be no superacceleration.

As is known, the Archimedes force acts upon the displaced fluid volume and is applied to its centroid. In our model, the centroid height $z_0(t)$ can be found from the definition

$$\int (z - z_0)\,\Delta\varrho\, dz d\mathbf{x} = 0,$$

where $\Delta\varrho(\mathbf{x},t)$ is the difference between densities of the jet and surrounding fluid.

Using the substitution $\Delta\varrho = \varrho_0\tau/g$, after integrating we find

$$z_0 = \frac{\frac{1}{2}\int \tau h^2 d\mathbf{x}}{\int \tau h d\mathbf{x}}. \tag{21}$$

Note that the numerator of this expression coincides with the potential energy in the Hamiltonian (3), while the denominator is the total buoyancy N. Thus, the centroid height depends not only on the shape h of the jet but also on its buoyancy τ.

Now let us check the lack of the superacceleration in our model. After substitution (9) into (21), and integrating over $\mathbf{x}$, we obtain

$$z_0 = \frac{2}{5}\frac{h_0}{\beta^2}. \tag{22}$$

Thus, using (19), from (22) it is easy to find that

$$z_0 = \tfrac{3}{5}A_0 g t^2. \tag{23}$$

The inequality $\frac{3}{5} < 1$ clearly demonstrates the lack of superacceleration for the centroid of the jet.

V. PLANE MODEL TESTING

For the numerical and analytical testing, it is more convenient to consider the one-dimensional (planar) version of the nonhydrostatic model, as the most simple, and to use Eqs. (1)–(2) in the Lagrangian representation.

The direct way to do this is to consider the parametrization $x = \hat{x}(s,t)$, where s is a new coordinate such that

$$\hat{x}_t = u|_{x=\hat{x}}, \quad \hat{h} = h|_{x=\hat{x}}, \quad \hat{\tau} = \tau|_{x=\hat{x}}.$$

Here and in the sequel the subscripts t and s will denote partial derivatives $f_t = \partial_t f$, $f_s = \partial_s f$.

In these notations, the planar version of Eqs. (1)–(2) rearranges to give

$$\hat{h}\hat{x}_{tt}\hat{x}_s + \partial_s\left(\tfrac{1}{2}\hat{h}^2\hat{\tau} + \tfrac{1}{3}\hat{h}^2\hat{h}_{tt}\right) = 0, \tag{24}$$

$$\partial_t(\hat{h}\hat{x}_s) = 0, \quad \hat{\tau}_t = 0. \tag{25}$$

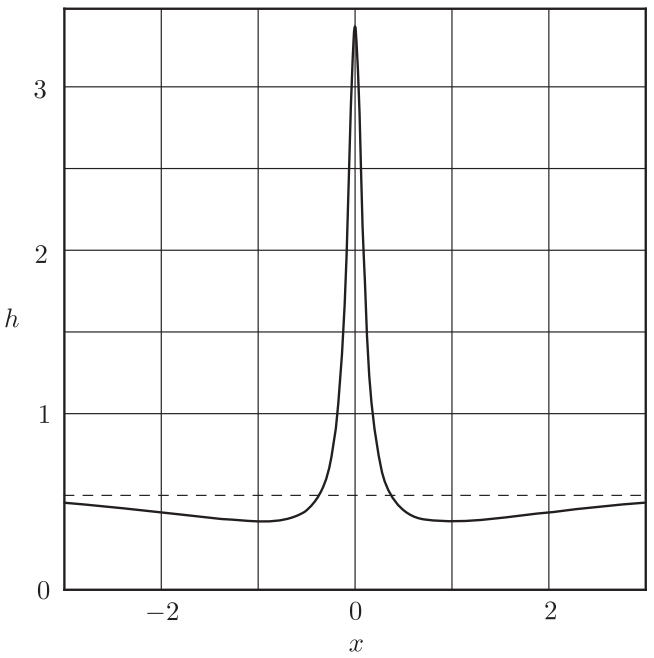

FIG. 6. Layer's surface elevation h as function of x at time $t = 25$.

Similar to the radial symmetric model, the planar one has also self-similar solutions

$$\hat{h} = \frac{a}{\beta}\sqrt{1 - s^2}, \quad \hat{\tau} = \frac{2}{3}ba\sqrt{1 - s^2}, \quad \hat{x} = a\beta s, \tag{26}$$

where $a > 0$ and b are some constants, $-1 \leqslant s \leqslant 1$, and the time-dependent variable β obeys the equation

$$\beta_{tt} = \frac{2\beta_t^2 + b\beta^3}{\beta(1 + \beta^4)}. \tag{27}$$

In the case $b < 0$ (as $t \to \infty$), Eq. (27) has the slower power-law asymptote

$$\beta \approx \frac{2}{|b|t^2} \tag{28}$$

compared with the radial symmetric model. Notwithstanding, on the base of the relationships

$$\hat{h}_{\max} = \frac{a}{\beta}, \quad \tau_0 = \frac{2}{3}ba = 2A_0 g,$$

which follows from (26) and (18), one can verify that the power law (28) leads to exactly the same result as (19).

In the general case when the problem (24), (25) is solved under arbitrary initial conditions

$$\hat{h}(s,0) = h_0(s), \quad \hat{x}(s,0) = s, \quad \hat{\tau}(s,0) = \tau_0(s), \tag{29}$$

the best way of solving is to use numerical methods.

For this, it is convenient to integrate Eqs. (25) and to introduce the displacement

$$\xi(s,t) = \hat{x}(s,t) - s, \tag{30}$$

as a new variable in terms of which we get the boundary-value problem

$$h_0\xi_{tt} + \partial_s\left(\frac{1}{2}\hat{h}^2\tau_0 + \frac{1}{3}\hat{h}^2\hat{h}_{tt}\right) = 0, \quad \hat{h} = \frac{h_0}{1 + \xi_s}. \tag{31}$$

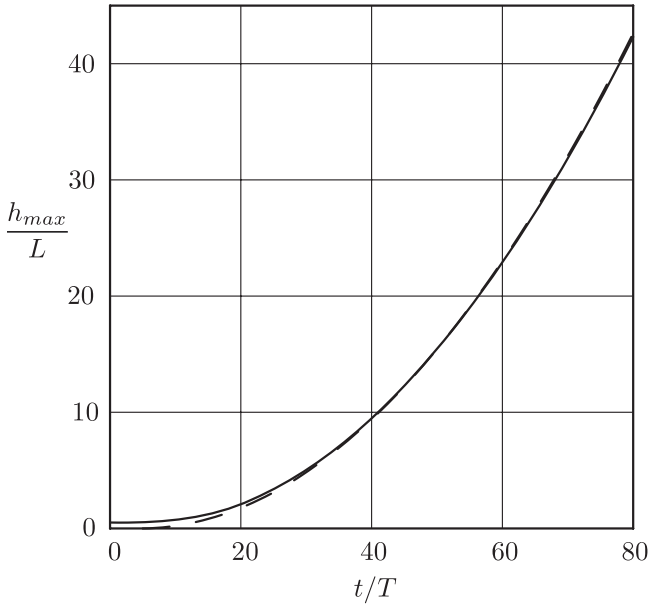

FIG. 7. Dependence of $h_{\max}$ on time. The dashed line corresponds to asymptotics (17), the solid line is calculated numerically.

In order to test the model's forecasting ability, we consider the problem (31), assuming the following initial conditions

$$h_0(s) = 0.5L, \quad \frac{\Delta\varrho}{\varrho_0} = 0.01 - \frac{0.02}{\cosh^2(s/L)}, \quad \xi_t(s,0) = 0,$$

where L and T are length and time scales linked as follows $L = gT^2$.

Thus, in the initial time $t = 0$, we have a layer with an alternating-sign relative buoyancy. Since a negative buoyancy is localized near $x = 0$, the central part of the layer must rise up, forming an upward jet as shown in Fig. 6.

According to Fig. 7, this process develops sufficiently quickly, and asymptotically (as $t/T > 20$) reaches the regime (17). It is interesting to note that the generation of the jet is accompanied by the shallowing effect, which manifests itself as profile concavities on either side of the jet. The dependence of $h_{\min}/L$ on time presented in Fig. 8 shows that the depth of cavities initially grows and then, after reaching the minimal value 0.2, slowly decreases.

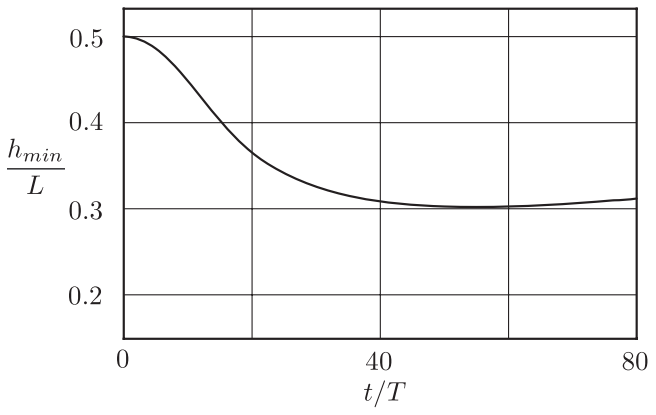

FIG. 8. Dependence of the shallowing level $h_{\min}$ on time.

VI. CONCLUSIONS

We now summarize the main results of the work. The main goal of this paper was to study the influence of nonhydrostaticity on the final stage of the Rayleigh-Taylor instability in the model of the active layer with horizontally nonuniform density.

As shown in this paper, the collapsing regime exists for both hydrostatic and nonhydrostatic models. However, in the latter models under the action of nonhydrostaticity the collapse slows down and at the final stage turns into the regime of algebraic instability. Actually, at this stage, the front of a narrow jet with negative relative buoyancy moves with uniform acceleration $3gA_0$, where A_0 is the peak value of the Atwood parameter. The superacceleration paradox is absent, because the centroid of the jet moves 2.5 times slower than its tip.

It is obvious that the model discussed above is an idealization. In particular, this model ignores such mechanisms as the Kelvin-Helmholtz instability or viscosity. Special attention should be given to these effects at the interface near the jet tip when its velocity becomes rather large. But the main limitation is the fact that evidently the model is applicable only to flows at which the horizontal density nonuniformity scale exceeds considerably the vertical one.

The used model is in need of additional testing because it presents a parametrization composed of terms dominant at the initial and final stage of the Rayleigh-Taylor instability. Nevertheless, the predictive power of the model is quite sufficient to describe some subtle phenomena. In particular, the nonhydrostatic model describes realistically enough the shallowing effect. This phenomenon manifests itself as profile concavities on either side of the jet coming out of the boundary layer due to the action of buoyancy force.

ACKNOWLEDGMENTS

This work was supported in equal parts by Russian Foundation for Basic Research (15-05-00854), by Presidium of Russian Academy of Sciences (Program "Fundamental Problems of Nonlinear Dynamics"), and by Russian Science Foundation (14-27-00134).

APPENDIX: SUBSTANTIATION OF MODEL

The governing equations for SW models in nonhydrostatic approximation can be derived directly from the complete fluid dynamics equations by traditional methods using the averaging procedure. However, for similar types of models, there exists a more simple and, most importantly, general method to obtain such equations from first principles (conservation laws).

This method is based on the Hamiltonian approach. In practice, in order to apply it to hydrodynamic models, which, just as (1), (2), evolve in the phase space of dynamic variables $\mathbf{u}, h, \tau$ the following steps must be taken in advance [28,34,35].

(i) Construct the energy functional $H[\mathbf{u},h,\tau]$ playing the role of the Hamiltonian.

(ii) Introduce the hydrodynamic momentum density $\mathbf{m}$, which obeys the variational relations

$$\mathbf{m} = \frac{\delta H}{\delta \mathbf{u}}, \quad \mathbf{u} = \frac{\delta H}{\delta \mathbf{m}}.$$

(iii) Specify the Poisson brackets, which in this case read as

$$\{m_i,m_k'\} = \partial_i'(m_k'\delta) - \partial_k(m_i\delta),$$
$$\{h,m_k'\} = -\partial_k(h\delta), \quad \{\tau,m_k'\} = -\delta\partial_k\tau.$$

Here and in what follows, primed field variables mean the dependence on the primed spatial coordinates, $\delta = \delta(\mathbf{x}-\mathbf{x}')$ is the Dirac δ function, and all the trivial Poisson brackets are omitted for the sake of space.

If the Hamiltonian $H[\mathbf{u},h,\tau]$ is given in explicit form, the corresponding equations of motion can be derived with the use of Poisson brackets and are written as

$$\partial_t m_i = \{m_i,H\} = -m_k\partial_i u_k - \partial_k(m_i u_k) - h\partial_i\frac{\delta H}{\delta h} + \frac{\delta H}{\delta\tau}\partial_i\tau, \tag{A1}$$

$$\partial_t h = \{h,H\} = -\partial_i\left(hu_i\right), \tag{A2}$$

$$\partial_t\tau = \{\tau,H\} = -u_i\partial_i\tau. \tag{A3}$$

The most creative step of the Poisson brackets method is the finding of the proper Hamiltonians. For some exact models, they are already known. Knowing them along with using approximation methods opens the way to deriving the Hamiltonians for new models.

As a basic model, we consider a two-layer ideal incompressible fluid, which moves under the action of gravity g between two rigid parallel planes $z=0$ and $z=l$ as shown in Fig. 1. Suppose the layers are separated by the interface $z=h(\mathbf{x},t)$ and have different densities. The upper layer has constant density ϱ_0, while the lower layer has density $\varrho = \varrho_0 + \Delta\varrho(\mathbf{x},t)$, where the density deviation $\Delta\varrho$, like h, is a time-dependent two-dimensional variable.

For simplicity, we assume also that the motion of a fluid in the upper layer is potential. Then by using the incompressibility condition and the continuity of the normal velocity component at the interface, as well as due to the rigid bottom condition, we obtain for the potential φ the following boundary-value problem:

$$\left(\Delta + \partial_z^2\right)\varphi = 0, \tag{A4}$$

$$\partial_z\varphi|_{z=l} = 0, \tag{A5}$$

$$\left(\mathbf{u} - \boldsymbol{\nabla}\varphi\right)_{z=h}\boldsymbol{\nabla}h = \left(w - \partial_z\varphi\right)_{z=h}, \tag{A6}$$

where Δ and $\boldsymbol{\nabla}$ are two-dimensional Laplacian and gradient operators, respectively, and $\mathbf{u}$ and w are horizontal and vertical velocity components in the lower layer.

Since the energy is an additive quantity, the total energy integral for this three-dimensional model consists of two summands:

$$H = H_1 + H_2, \tag{A7}$$

$$H_1 = \frac{1}{2}\int_h^l \varrho_0[(\nabla\varphi)^2 + (\partial_z\varphi)^2 + 2gz]dzd\mathbf{x}, \tag{A8}$$

$$H_2 = \frac{1}{2}\int_0^h \varrho(\mathbf{u}^2 + w^2 + 2gz)dzd\mathbf{x}, \tag{A9}$$

Here H_1 and H_2 are the total energies for the upper layer and the lower layer, respectively.

The simplest SW model can be derived under the hypothesis of hydrostatic equilibrium. This condition allows us to neglect the vertical velocity w in comparison with the horizontal one $\mathbf{u}$, assuming that $\mathbf{u}$ is dependent only on $\mathbf{x}$ and t. It is such minimal model that was studied in Refs. [9–11].

Let now the hydrostaticity condition be not fulfilled so that $w \neq 0$, and let $\mathbf{u}$ be nearly independent of z as before. Then from the divergence-free condition

$$\partial_z w + \boldsymbol{\nabla}\cdot\mathbf{u} \approx 0, \tag{A10}$$

and the edge condition $w|_{z=0} = 0$, we have

$$w \approx -z\boldsymbol{\nabla}\cdot\mathbf{u}. \tag{A11}$$

This relation must be treated as one of the possible parametrizations. In particular, it would be possible to consider the other parametrization

$$\mathbf{u} = \frac{z}{h}\mathbf{v}, \quad w = -\frac{z^2}{2}\boldsymbol{\nabla}\cdot\left(\frac{\mathbf{v}}{h}\right),$$

where $\mathbf{v}(\mathbf{x},t)$ is treated as horizontal velocity at the boundary surface, i.e., $\mathbf{v} = \mathbf{u}|_{z=h}$.

On the one hand, such parametrization implies a linear z dependence of the vertical profile of the horizontal velocity $\mathbf{u}$, but, on the other hand, it will lead to a more intricate model. Thus, the choice of parametrization depends on the physical and model assumptions. We restrict ourselves to the parametrization (A11), which corresponds to a minimum model and is suitable for researching the influence of nonhydrostaticity at a qualitative level.

One can suggest a way to the construction of more general parametrizations. Let the horizontal velocity $\mathbf{u}$ be dependent on z as

$$\mathbf{u} = F\left(\frac{z}{h}\right)\mathbf{v},$$

where $F(z)$ is a function of z. Then from the incompressibility condition (A10) it follows that

$$w = \frac{z}{h}F\left(\frac{z}{h}\right)(\mathbf{v}\cdot\boldsymbol{\nabla})h - Q\left(\frac{z}{h}\right)\boldsymbol{\nabla}\left(h\mathbf{v}\right),$$

where $Q(z)$ is the function defined as $dF/dz = Q$.

Using the approximation (A11) and putting without loss of generality $\varrho_0 = 1$, after integration over z, we obtain from (A7)–(A9) to the main order in $\Delta\varrho/\varrho_0 \ll 1$

$$H = \frac{1}{2}\int\left(h\mathbf{u}^2 + h^2\tau + \frac{1}{3}h^3(\boldsymbol{\nabla}\cdot\mathbf{u})^2 + \varphi|_{z=h}\boldsymbol{\nabla}\cdot(h\mathbf{u})\right)d\mathbf{x}, \tag{A12}$$

where the relative buoyancy $\tau = g\Delta\varrho/\varrho_0$, in contrast to h, is a sign-alternating quantity.

Eliminating from (A12) all terms except for the two first ones gives the Hamiltonian corresponding to the so-called minimal model [9–11]. The third term is the Green-Naghdi correction responsible for the effect of nonhydrostaticity. The last correction is nothing other than a result of the reaction to the potential flow in the upper layer. Thus in the context of the two-layer model the use of the truncated Hamiltonian without

the last correction term is justified if only the dynamical influence of the upper layer can be ignored. To provide the motivation for such truncation procedure, we estimate the contribution of the last term for two various flow regimes. One of them is long-wave motions while the other is a self-similar collapse.

To do this we recast the boundary-value problem (A4)–(A6) in the form

$$\left(\Delta + \partial_z^2\right)\varphi = 0, \tag{A13}$$

$$\partial_z\varphi|_{z=l} = 0, \tag{A14}$$

$$[(\nabla\varphi)\nabla h - \partial_z\varphi]_{z=h} = \nabla\cdot(h\mathbf{u}) = -\partial_t h. \tag{A15}$$

Above all, we consider the long-wave regime. Let L be the horizontal length scale and U be the scale of the velocity. Depending on whether the scale L is much greater or much less than l, the boundary-value problem (A13)–(A15) leads to two approximations

$$\varphi|_{z=h}\nabla\cdot(h\mathbf{u}) \approx \begin{cases} \dfrac{1}{l}\left(\hat{G}\partial_t h\right)^2, & \text{if } L \gg l \gg h, \\ (\partial_t h)\,(\hat{G}\partial_t h), & \text{if } l \gg L > h, \end{cases} \tag{A16}$$

where $\hat{G}$ is the integral operator

$$\hat{G}f = \int \frac{f(\mathbf{x}')}{|\mathbf{x}-\mathbf{x}'|}d\mathbf{x}'.$$

Since $h\mathbf{u}^2$ is of the order hU^2, it is this term that gives the main contribution in the long-wave approximation in comparison with terms (A16), which have the order h^2U^2/l and h^2U^2/L, respectively.

In order to make estimations for the collapsing regime, it is handier to consider the approximation $l \to \infty$. In this case, the potential φ can be expressible as

$$\varphi = -\partial_z \int \frac{\Phi(\mathbf{x}',t)d\mathbf{x}'}{\sqrt{z^2 + (\mathbf{x}-\mathbf{x}')^2}}, \tag{A17}$$

through the double-layer potential $\Phi(\mathbf{x},t)$ in terms of which the boundary problem (A13)–(A15) is written as

$$\nabla\cdot\int \frac{h\nabla'\Phi(\mathbf{x}',t)d\mathbf{x}'}{[h^2(\mathbf{x},t) + (\mathbf{x}-\mathbf{x}')^2]^{3/2}} = -\nabla\cdot(h\mathbf{u}) = \partial_t h(\mathbf{x},t). \tag{A18}$$

Under the assumption of self-similarity, it is natural to suggest that each of the variables $\varphi|_{z=h}$, h, $\mathbf{u}$, Φ can be factorized as

$$\varphi|_{z=h} = \mu\tilde{\varphi}, \quad \Phi = \kappa\tilde{\Phi}, \quad h = \beta^{-2}\tilde{h}, \quad \mathbf{u} = \alpha\tilde{\mathbf{u}}, \tag{A19}$$

where μ, κ, β, α are time-dependent factors, and $\tilde{\varphi}$, $\tilde{\Phi}$, $\tilde{h}$, $\tilde{\mathbf{u}}$ are functions depending only on the self-similar argument $\mathbf{x}/\beta$. Then the direct substitution of (A19) in (A17) and (A18) gives, in the limit as $\beta \to 0$, the relations

$$\mu = \alpha\beta, \quad \kappa = \alpha\beta^{-5}, \quad \alpha = \partial_t\beta,$$

which allow us to obtain asymptotic estimates

$$\varphi|_{z=h}\nabla\cdot(h\mathbf{u}) \sim \alpha^2\beta^{-2},$$
$$h\mathbf{u}^2 \sim \alpha^2\beta^{-2}, \quad h^3(\nabla\cdot\mathbf{u})^2 \sim \alpha^2\beta^{-8}.$$

Thus, the integrand responsible for the influence of the upper layer does not dominate in any of the regimes. The variations caused by the third term are compensated by either the first term or the second one depending on the regime. This fact provides the motivation for the truncation procedure, which allows us to drop the last term in (A12) and to obtain the so-called Hamiltonian of an active layer

$$H = \frac{1}{2}\int\left(h\mathbf{u}^2 + \frac{1}{3}h^3(\nabla\cdot\mathbf{u})^2 + h^2\tau\right)d\mathbf{x}.$$

The application of the Poisson brackets method to this Hamiltonian yields Eqs. (1), (2). To be convinced of this, in a way similar to Refs. [16,37], we need first of all to find the momentum density

$$\mathbf{m} = \frac{\delta H}{\delta\mathbf{u}} = h\mathbf{u} - \frac{1}{3}\nabla\left(h^3\nabla\cdot\mathbf{u}\right), \tag{A20}$$

from which it is easy to derive that

$$\mathbf{m}\cdot\delta\mathbf{u} = \mathbf{u}\cdot\delta\mathbf{m} - (\mathbf{u}^2 + h^2(\nabla\cdot\mathbf{u})^2)\delta h + \cdots. \tag{A21}$$

The notation $\cdots$ implies that the equality holds up to divergence terms, which give zero contributions on integration over space thanks to proper boundary conditions.

Considering (A20) as a constraint, we obtain with use of (A21) the variational equality

$$\begin{aligned}\delta H &= \delta\left(\frac{1}{2}\int(\mathbf{u}\cdot\mathbf{m} + h^2\tau)d\mathbf{x}\right) \\ &= \int\left((h\tau - \frac{1}{2}\mathbf{u}^2 - \frac{1}{2}h^2(\nabla\cdot\mathbf{u})^2)\delta h\right. \\ &\quad \left. + \mathbf{u}\cdot\delta\mathbf{m} + \frac{1}{2}h^2\delta\tau\right)d\mathbf{x},\end{aligned} \tag{A22}$$

whence we have

$$\frac{\delta H}{\delta\tau} = \frac{1}{2}h^2, \quad \frac{\delta H}{\delta\mathbf{m}} = \mathbf{u}, \tag{A23}$$

$$\frac{\delta H}{\delta h} = -\frac{1}{2}\mathbf{u}^2 - \frac{1}{2}h^2(\nabla\cdot\mathbf{u})^2 + h\tau. \tag{A24}$$

Substituting (A20), (A23), and (A24) in Eqs. (A1)–(A3), after some manipulation, leads to Eqs. (1), (2).

[1] S. I. Abarzhi, Phil. Trans. R. Soc. A **368**, 1809 (2010).
[2] S. I. Abarzhi, Phys. Scr. T **132**, 014012 (2008).
[3] H. J. Kuhl, Phys. Rep. **206**, 197 (1991).
[4] K. O. Mikaelian, Phys. Rev. E **89**, 053009 (2014).
[5] N. J. Mueschke, M. J. Andrews, and O. Schilling, J. Fluid Mech. **567**, 27 (2006).

[6] N. J. Mueschke and O. Schilling, Phys. Fluids **21**, 014106 (2009).
[7] N. J. Mueschke and O. Schilling, Phys. Fluids **21**, 014107 (2009).
[8] S. Chandrasekhar, *Hydrodynamic and Hydromagnetic Instability* (Clarendon Press, Oxford, 1961).
[9] V. P. Goncharov and V. I. Pavlov, JETP Lett. **96**, 427 (2012).
[10] V. P. Goncharov and V. I. Pavlov, Phys. Rev. E **88**, 023002 (2013).
[11] V. P. Goncharov and V. I. Pavlov, JETP **117**, 754 (2013).
[12] D. H. Peregrine, J. FIuid Mech. **27**, 815 (1967).
[13] A. E. Green and P. M. Naghdi, J. Fluid Mech. **78**, 237 (1976).
[14] T. Y. Wu, J. Eng. Mech. Div., Proc. ASCE **107**, 501 (1981).
[15] R. Camassa and D. D. Holm, Physica D **60**, 1 (1992).
[16] R. Camassa, D. D. Holm, and J. M. Hyman, Adv. Appl. Mech. **31**, 1 (1994).
[17] V. P. Goncharov and V. I. Pavlov, JETP Lett. **84**, 384 (2006).
[18] V. P. Goncharov, JETP **105**, 1075 (2007).
[19] V. P. Goncharov and V. I. Pavlov, Phys. Rev. E **76**, 066314 (2007).
[20] V. P. Goncharov, JETP Lett. **89**, 393 (2009).
[21] V. P. Goncharov and V. I. Pavlov, JETP **111**, 124 (2010).
[22] V. P. Goncharov, JETP **113**, 714 (2011).
[23] M. Hirota, T. Tatsuno, and Z. Yoshida, J. Plasma Phys. **69**, 397 (2003).
[24] N. A. Inogamov, A. Yu. Demyanov, and E. E. Son, *Hydrodynamics of Mixing* (Publishing House of the Moscow Physico-Technical Institute, Moscow, 1999) (in Russian).
[25] V. E. Zakharov and E. A. Kuznetsov, Phys. Usp. **55**, 535 (2012).
[26] E. Fermi, in *Collected Papers of Enrico Fermi* (University of Chicago Press, Chicago, 1965), Vol. II, ch. 244, p. 816.
[27] E. Fermi, in *Collected Papers of Enrico Fermi* (University of Chicago Press, Chicago, 1965), Vol. II, ch. 245, p. 821.
[28] V. P. Goncharov and V. I. Pavlov, *Hamiltonian Vortex and Wave Dynamics* (Geos, Moscow, 2008) (in Russian).
[29] "Ockham's razor", Encyclopædia Britannica, Encyclopædia Britannica Online, 2010. Retrieved 12 June 2010.
[30] G. I. Barenblatt, *Scaling, Self-Similarity, and Intermediate Asymptotics* (Cambridge University Press, Cambridge, 1996).
[31] V. P. Goncharov and V. I. Pavlov, JETP Lett. **90**, 317 (2014).
[32] P. Ripa, Geophys. Astrophys. Fluid Dyn. **70**, 85 (1993).
[33] P. J. Dellar, Phys. Plasmas **9**, 1130 (2002).
[34] V. P. Goncharov and V. I. Pavlov, *Problems of Hydrodynamics in the Hamiltonian Description* (Moscow University Press, Moscow, 1993) (in Russian).
[35] V. P. Goncharov and V. I. Pavlov, Eur. J. Mech., B/Fluids **16**, 509 (1997).
[36] S. V. Bazdenkov, N. N. Morozov, and O. P. Pogutse, Dokl. Akad. Nauk SSSR **293**, 818 (1985) [Sov. Phys. Dokl. **32**, 262 (1987)].
[37] D. D. Holm, Phys. Fluids **31**, 2371 (1988).